3D Biomechanical Modeling of the Human Diaphragm Based on CT Scan Images

H. Ladjal[1,2], J. Saade[1], M. Beuve[2], J. Azencot[1], J-M. Moreau[1] and B. Shariat[1]

[1] LIRIS CNRS UMR 5205, Université Claude Bernard Lyon 1, France
[2] IPNL CNRS UMR 5822, F-69622, Université Claude Bernard Lyon 1, France

Abstract— **Predicting respiratory motion is challenging, due to the complexity and irregularity of the underlying motion pattern. In order to predict respiratory motion, we have developed a biomechanical modeling of the respiratory system which utilizes the 4D scan data (geometrical and mechanical properties) to accurately predict the tumor position due to the deformations and displacement caused by the respiratory movement, to increase the precision of the treatment. The diaphragm is the principal muscle used in the process of respiration. In this case, we introduce a method that enables the simulation of the contractile force generated by the diaphragm muscles. Physiologically, respiratory motion modeling involves the use pressure-volume relationship to apply pressure loading on the surface of the diaphragm. Additionally, the real diaphragm boundary conditions are included to the model and simulated responses are compared to clinical data. Finally, these comparisons show the effectiveness of the proposed physically-based model.**

Keywords— **Finite element modeling, Biomechanics, Human diaphragm anatomy, Medical images, Hadrontherapy.**

I. Introduction

Hadrontherapy is an advanced radiotherapy technique for cancer treatment. It offers a better irradiation ballistic than conventional techniques and requires an appropriate quality assurance procedures. Tumor motion during irradiation reduces target coverage and increases dose to healthy tissues. Prediction of respiratory motion has the potential to substantially improve cancer radiation therapy. The respiratory motion is complex and its prediction is not a simple task, especially that breathing is controlled by the independent action of the thorax and diaphragm muscles. Current techniques based on imaging, such like Cone-Beam or deformable image registration, attempt to predict the position of lung tumors [1]. Unfortunately, these methods assume a reproducible movement of the respiratory system. Also, these methods are risky and/or invasive, and do not compute the evolution of the surrounding organs, which is essential information to determine the position of the Bragg peak. Therefore, motion prediction of the tumor from simple sets of medical images appears to be insufficient. However, the complete simulation of the respiratory dynamics requires the simulation of the diaphragm motion during respiration. The diaphragm is the principal muscle of respiration. Studying his shape and motion are great importance in order to detect respiratory diseases and study the induced motion of other organs in the thorax and abdomen for radiotherapy. Various models have been implemented, the diaphragm modeling are usually derived using either mass-spring approach or finite element method. The models that are most known and used by the graphic community are based on the mass-spring methods, which are often used for real time applications within graphic simulators [2], [3]. However, these models have certain drawbacks: the exacte relationship between the physical parameters of the organs and coefficients of stiffness of the springs cannot be computed. Behr et al. [4] propose a virtual model including global deformation of the diaphragm based on the finite element model HUMOS. The model is based on a linear function of muscle contraction (excitation). Unfortunately, the authors do not elaborate the mechanical behavior of the diaphragm. [5] proposed the incompressible transversely isotropic hyperelastic model. Their geometric model is obtained by segmentation of the diaphragm (old female cadaver), then this geometry is subject to an excitation function assuming a reproducible movement, compatible with their targets for diagnosis and study of certain diseases. Unfortunately, the behavior obtained from this model is not confronted with clinical data. In this paper, we illustrate an alternative approach consisting on the development of a biomechanical model of human diaphragm based on CT-scan data. In order to be accurate, the model must include the variability of respiratory motion, the rib cage, the diaphragm and the lungs behaviors, and should be correlated and controlled by external non-invasive parameters.

II. Anatomical model

The diaphragm is a dome-shaped musculofibrous membrane which separates the thorax from the abdominal cavity. It presents the shape of a dome concave toward the abdomen (Fig.2). It is composed of a peripheral part (muscular fibre) and a central part (tendon). The tendon is the upper part of the diaphragm, in contact with the lungs and is closer to the front than to the back of the thorax, so that the posterior muscular fibres are longer [6]. In structure, the central tendon

M. Long (Ed.): World Congress on Medical Physics and Biomedical Engineering, IFMBE Proceedings 39, pp. 2188–2191, 2013.
www.springerlink.com

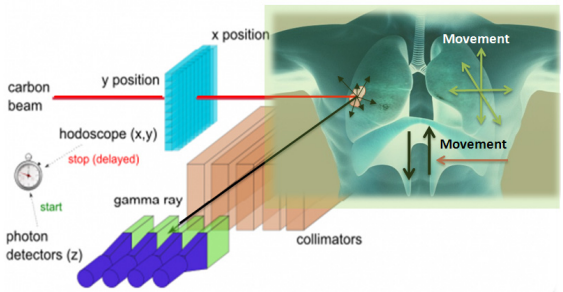

Fig. 1: Hardotherapy: radiation treatment for lung cancer using the carbon ions to simulate the dose deposition.

is composed of several planes of fibres, whose arrangement give strength and rigidity. The peripheral part, which consists of muscles, is linked to the lower thoracic cavity perimeter and has three major insertions: lumbar, sternum and ribs.

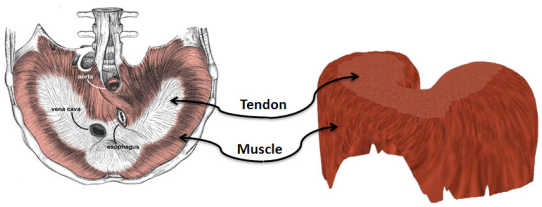

Fig. 2: Anatomy of the respiration system: ribs, the diaphragm (tendon + muscle), the lungs and the mediastinum.

III. Methodology

Fig.3 shows our approach for validating finite element computational models. The mechanical and geometrical properties are injected in the simulation finite element. The deformations of the human diaphragm are measured using a patient's CT scan images and compared to the personalized finite element model's predicted results.

A. Building the 3D geometrical model

In order to build a patient specific biomechanical model of the diaphragm, a parametric patient-specific geometrical model is generated from a 4D CT image. To validate the biomechanical model, at least two data sets corresponding to two different respiratory phases should be provided. We build a geometrical model at normal full exhalation and another at full inhalation, then we evaluate the developed biomechanical model ability to predict this motion. In this order, we have chosen CT scan data covering the whole thorax of a patient. The 4D CT set is issued from a pre-treatment procedure of a lung cancer patient. From the 4D set, we choose

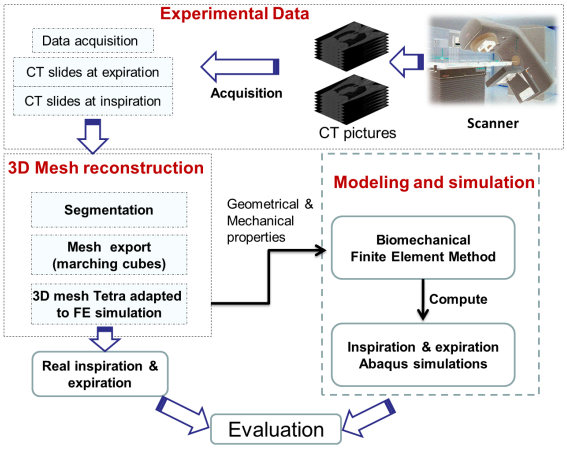

Fig. 3: Approach for validating finite element computational models: from the CT images to the biomechanical model.

two 3D sets of images that correspond to the maximum and to the minimum of the respiratory cycle. In terms of resolution, the CT images voxel size is $1.17 \times 1.17 \times 3$ mm^3 with $512 \times 512 \times 130$ voxels respectively in the left-right (X), dorsoventral (Y) and craniocaudal (Z) directions.

B. CT images segmentation

The diaphragm was segmented using the snake evolution methodology available within ITK-SNAP library (Fig.4). The diaphragm muscles and tendon cannot be identified separately on the CT images, neither visually nor automatically. According to [7] that used information from [8], the mean central tendon surface area is 143 cm^2. This area does not vary to a large degree between one person and another.

IV. Biomechanical Model

The respiratory system is an extremely complicated structures from a biomechanical point of view. The linear elasticity is often used for the modeling of deformable materials, mainly because the equations remain quite simple and the computation time can be optimized. The physical behavior of soft tissue may be considered as linear elastic if its displacement and deformation remain small (less than 10% of the mesh size). In this section we presents a personalized biomechanical modeling where the diaphragm is considered as compressible solid with an elastic behavior, and as a heterogeneous material with the muscles in peripheral part and the tendon in central part. The muscles of the diaphragm are skeletal muscle type. The action of skeletal muscles have the effect of shortening or lengthening the muscles in a direction

parallel to muscle fibers.

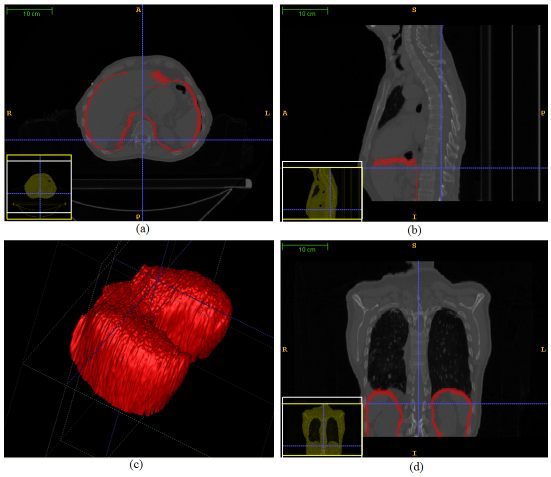

Fig. 4: User interface of the segmentation tool: human diaphragm.

A. *Elastic finite element model*

For an isotropic elastic material the elastic energy, noted W, can be written as:

$$W(\mathbf{E}) = \frac{\lambda}{2}\left(tr\mathbf{E}\right)^2 + \mu\, tr\left(\mathbf{E}^2\right) \tag{1}$$

where $\mathbf{E}$ is the Green-Lagrange strain tensor λ and μ are the Lame's coefficients

$$\begin{aligned}\mathbf{E} &= \frac{1}{2}(\mathbf{F}^T.\mathbf{F}-\mathbf{I}) \\ &= \tfrac{1}{2}\left(\mathbf{grad}\,\underline{U} + \mathbf{grad}^T\,\underline{U} + \mathbf{grad}^T\,\underline{U}.\mathbf{grad}\,\underline{U}\right)\end{aligned} \tag{2}$$

A displacement based finite element solution is obtained with the use of the principal of virtual works. For small deformations, the Green-Lagrange strain tensor is linearized into the infinitesimal strain tensor:

$$\varepsilon = \frac{1}{2}(\mathbf{grad}\,\underline{U} + \mathbf{grad}^T\,\underline{U}) \tag{3}$$

The relation between the Cauchy stress tensor and the linearized strain tensor is written with Lame's coefficient in condensed vector notation as :

$$\sigma = \lambda\,(tr\,\varepsilon)\,\mathbf{I} + 2\,\mu\,\varepsilon \tag{4}$$

where $\mathbf{I}$ is the identity matrix.

Surface tension models generate forces that only depend in amplitude on the surface area of the geometrical model.

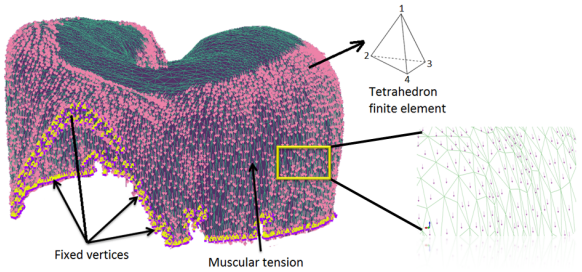

Fig. 5: The boundary conditions applied to the mesh nodes with the diaphragm attached to the periphery (yellow) and muscle tension (purple).

When applying the tension $\overrightarrow{t_s}$ on the diaphragm muscles mesh, the resulting force can be written as:

$$\overrightarrow{f} = \int_S \overrightarrow{t_s}\, dS = \alpha \int_S \overrightarrow{dir_s}\, dS \tag{5}$$

with S, α et $\overrightarrow{dir_s}$ respectively the mesh surface, the force amplitude and direction. The Fig.5 presents the radial direction forces muscle from the tendon, which corresponds anatomically to the direction of muscle fibers [5]. The boundary conditions are inferred from the anatomy.

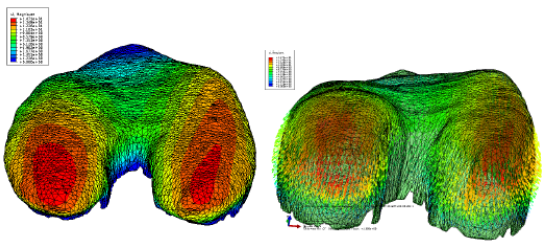

Fig. 6: Finite element simulation of the human diaphragm: deformation and von Mises distribution.

V. Experiments and Validation

In order to demonstrate the validity of the proposed FEM, we have compared the results of a simulated diaphragm motion with the experimental data provided by the CT scan images. The mechanical and geometrical properties used in our finite element simulations are settled in Table.1. Firstly, we have investigated stress distribution and total deformation of the diaphragm during normal inspiration (Fig.6). We can see the maximum stress is generated at the right-posterior and left-posterior sides, also we notice a slightly larger motion to the right than to the left sides. Then, we used a local metric that measures the Euclidean distance between simulated and experimental meshes. Fig.7 presents a 3D distance map

Table 1: Mechanical and geometrical properties of the diaphragm

	Tendon	*Muscles*	*all*
$E(MPa)$	33	5.32	-
ν	0.3	0.3	-
Vertices	6365	9966	15411
Tetra	27671	35348	63019
$Surf(\text{mm}^2)$	18220,34	92806,84	111027,18
$Vol(\text{mm}^3)$	1192258.64	468519.19	660777.81

measured from each node of the real diaphragm at inspiration to the nodes of the simulated inspiration. The simulations show that the developed finite element model is in good agreement with our experimental data (Fig.8). To improve the precision of our biomechanical simulation, the comparison have been calculated between the mesh volume of the simulated diaphragm and real segmented mesh based in CT scan images, the volume errors are less than 3.9% (Table.2), these errors depend mainly on the quality of the 3D segmentation.

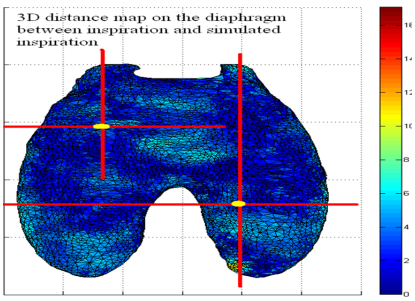

Fig. 7: 3D mapping distances: the finite element simulation versus the experimental inspiration.

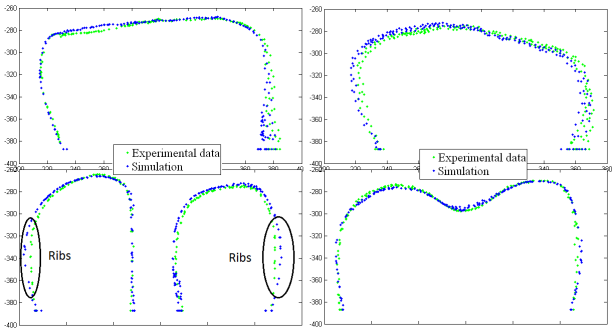

Fig. 8: Comparison between the simulation and clinical inspiration.

Table 2: Volume variation between experimental data and simulation data

Inspiration state	Volume
V_1 $(experimental)$ mm^3	2830880.530272
V_2 $FEM\ Simulation$ mm^3	2721523.983245
Error V %	3.86 %

VI. Conclusion

We have developed a biomechanical model to simulate a respiratory system. We first investigated the challenging issues in biomechanical modeling of the human diaphragm. The deformation of the diaphragm is quite realistic compared to experimental data. We can see clearly that the proposed physically-based FEM model is able to simulate the diaphragm deformation. Currently, we are working on integrating the diaphragm behavior in our realistic biomechanical model of the respiratory system including the behavior of the lungs, pleura, thorax and soft tissues behaviors. Furthermore, theses simulations will be coupled with the kinematic modeling of the ribcage to correlate external/internal movements.

Acknowledgements

This research is supported by the ENVISION project (co-funded by the European Commission under the FP7 Collaborative Projects Grant Agreement Nr. 241851FP7), and by ETOILE's Research Program (PRRH/UCBL, under CPER 2007-13 funding).

References

1. H. Shirato, K. Suzuki, GC. Sharp, et al. Speed and amplitude of lung tumor motion precisely detected in four-dimensional setup and in real-time tumor-tracking radiotherapy *International Journal of Radiation Oncology Biology Physics.* 2006;Volume 64, Issue 4:1229-1236.
2. Promayon E., Baconnier P.. A 3D discrete model of the diaphragm and human trunk in *ESAIM: Proceedings*;23:66-77 2008.
3. Villard P.F., Bourne W., Bello F.. Interactive simulation of diaphragm motion through muscle and rib kinematics in *Recent Advances in the 3D Physiological Human, Springer London*:91-103 2009.
4. Behr M., Prs J., Llari M., Godio Y., Jammes Y., Brunet C.. A three-dimensional human trunk model for the analysis of respiratory mechanics *Journal of biomechanical engineering.* 2010;132:014501-1-014501.
5. Pato M.P.M., Santos N.J.G., Areias P., et al. Finite element studies of the mechanical behaviour of the diaphragm in normal and pathological cases *Comput Methods Biomech Biomed Engin.* 2011;14(6):505-513.
6. Gray Henry. *Gray's Anatomy*. Running Press 1974.
7. Cluzel P., Similovsky T., Chartrand-Lefebvre C., Zelter M., Derenne J.-P., Grenier P.. Diaphragm and chest wall: Assessment of the inspiratory pump with MR imaging - Preliminary observations *Radiology.* 2000;215:574-583.
8. Arora N., Rochester D.. Effect of body weight and musculatory on human diaphragm muscle mass, thickeness, and area *J Appl Physiol.* 1982;52:64-70.